UNIVERSITI
TEKNOLOGI
PETRONAS

To Study the Effect of Nanoparticle Loadings and Effect of Alternative Base FluidsTowards Improvements in Drilling Fluid Properties

by

Chai Yee Ho

13721

Dissertation submitted in partial fulfilment of the requirements of for the Bachelor of Engineering (Hons.) (Chemical)

MAY 2014

Universiti Teknologi PETRONAS
Bandar Seri Iskandar
31750 Tronoh
Perak Darul Ridzuan

CERTIFICATION OF APPROVAL

To Study the Effect of Nanoparticle Loadings and Effect of Alternative Base Fluids Towards Improvements in Drilling Fluid Properties

by

Chai Yee Ho
13721

A project dissertation submitted to the

Chemical Engineering Programme

Universiti Teknologi PETRONAS

in partial fulfilment of the requirement for the

BACHELOR OF ENGINEERING (Hons.)

(CHEMICAL)

Approved by,

_____

(AP Dr.SuzanaYusup)

UINVERSITI TEKNOLOGI PETRONAS

TRONOH, PERAK

MAY, 2013

CERTIFICATION OF ORIGINALITY

This is to certify that I am responsible for the work submitted in this project, that the original work is my own except as specified in the references and acknowledgements, and that the original work contained herein have not been undertaken or done by unspecified sources or persons.

_____

CHAI YEE HO

ABSTRACT

Nanotechnology is increasing capturing the attention of material researches as this technology pushes the limits and boundaries of the pure material itself. Various material enhancement can be done through nanotechnology and drilling fluid for oil and gas explorations are no exceptions as well. Through this paper, it is desired to study the effect of alternative base fluids for the current conventional base fluid but with the addition of nanoparticles. Besides that, it is desired to study the effect of multiple nanoparticles loadings into base fluid to determine the value of enhancements to the base fluid. Researchers had conducted various experiments of nanoparticles dispersion into individual fluids which are unrelated to drilling mud and also into water-based drilling mud. However, no studies had been conducted as said for comparison of different base fluids at different nanoparticle loadings. This spurs the intention of this paper to investigate the effects of the said scenario.

ACKNOWLEDGEMENTS

The author would like to express his sincere gratitude and deep appreciation to the following people for their support, patience and guidance. Without them, this project wouldn't have been made possible. It is to them that the author owing them his gratitude.

- AP Dr Suzana Yusup for the continuous advice, guidance, constructive criticism and support to the author. Despite her heavy workload, she spared her precious time to discuss on the project.
- Mdm. Ruzaimah Binti Nik Mohamad Kamil as co-supervisor for the advice and suggestions given throughout this project
- Platinum NanoChemicals Sdn. Bhd. for the contributions of carbon nanoparticle and base fluid materials to make this project a reality.
- Lab technicians from various labs for the guidance and help rendered throughout this project.

Finally, above all, the author would also like to thank his family, friends and Chemical Engineering Department lecturers for their unwavering, love, support and assistance throughout the project, Not to forget, special thanks to Universiti Teknologi PETRONAS for providing him laboratory facilities to run the experiments and analysis.

TABLE OF CONTENTS

List of Figures

List of Tables

CHAPTER 1

INTRODUCTION

1.1 Background

Drilling fluid, commonly known as drilling mud, is one of the most important aspects in any drilling process. It is required in a wellbore, a hole that is drilled for the aid of excavation of natural resources including oil, gas or water("Wellbore,"). Drilling fluid primarily aids to cool and lubricate the drilling bit, remove solid fragments from drilling area to the surface and counterbalancing the formation pressure within the wellbore("Functions of a Drilling Fluid ", 2012).

Appropriate heat transfer and fluid flow characteristics is imperative in any types of drilling mud. Additives are often added to maintain the density, rheology and temperature stability of drilling muds. Deep hole drilling is often conducted in an environment with high temperature and pressure which poses problems to drilling equipment used. Such problems include overheating of equipment as well as lost circulation are common in any drilling operations due to the limitations posed by drilling mud. Therefore, it is required to further enhance the current drilling mud properties to adapt to harsher surroundings in any drilling operations.

Such enhancement can be done through the introduction of nanotechnology where nanoparticles are introduced to increase thermal conductivities and rheological properties of the drilling fluid.

A nanofluid is a dilute suspension of metallic or non-metallic nanomaterials with a typical size of equal or less than 100 nm in a base liquid. In recent years, the addition of nanoparticles have proven to be benefitting the usages of other fluids such as engine oil fluid. The additions of nanoparticles have been studied ever since its discovery to have significantly high thermal conductivities. Such property is essential in the production of drilling fluid as drilling muds must be able to withstand high temperature and high rheological changes to avoid unstable and decomposition of the drilling mud properties.

Common oil-based muds includes the usage of diesel oil are used as drilling fluids as it minimizes the swelling of clay within the reservoir and reduces the

wettability of the formation. Due to high initial cost, oil palm based is more preferable as it is more cost effective and pose less environmental pollutions. Therefore, alternative base fluids for drilling mud such as methyl ester, renewable fuel and base oil is proposed to replace the conventional drilling muds.

1.2 Problem Statement

A common drilling mud types used in drilling operations are water-based mud, oil-based mud and synthetic-based fluid. Due to higher cost of production, water-based and oil-based mud are more preferable. However, limitations of thermal properties in both mud types has posed difficulties in deep hole drilling operations.

Such issue must be overcome through the enhancements of drilling fluid properties through the introduction of nanotechnology.

1.3 Objectives and Scope of Study

1.3.1 Objective

The objective of this study is to study the effects of addition of different functionalized graphene oxide nanoparticle loadings into alternative base fluids to produce drilling nanofluid apart from the conventional choices of types of base fluids for drilling mud.

1.3.2 Scope of Study

The scope of study is segregated into few categories:

1. The study of physical properties of alternative base fluids to determine its suitability as base fluid for drilling mud usage.
2. To study the effects of functionalized graphene oxide addition in terms of rheological and thermal properties of the drilling mud.
3. To study the methods of equal distribution dispersions of functionalized graphene oxide into the base fluid.

CHAPTER 2

LITERATURE REVIEW AND THEORY

2.1 Introduction

Based on ScienceDaily, nanoparticle is defined as "a microscopic particle with at least one dimension less than 100 nm." Nanoparticles is found to have intense potential in variety of applications which alters the physical properties of certain materials in nanoscale. The properties changes as the size of particles approaches nanoscale.

Liquids suspended with nanoparticles are termed "nanofluids". Nanofluids usually show immense enchancement of their properties due to the presence of nanoparticles which affects the properties of the fluid itself. However, many publications concerned with nanofluids have been found to possess enhancement in terms of thermophysical properties such as thermal conductivity, thermal diffusivity, viscosity and convective heat transfer coefficients compared to base fluid such as oil and water (Wong & Leon, 2009).

In recent years, nanotechnology is starting to make its impact globally through further expanding the current limitations of various materials being used and practised in everyday activities. The properties of materials are differentiated to the conventional material used in nanoscale as nanomaterials have a relatively larger surface area when compared to materials produce in larger of the same mass. This enhances the material as they are chemically more active and enhancement in terms of strength, electrical and thermal properties can be seen(Hashim, Nadia, & Salleh, 2009).

The integration of nanotechnology into oil and gas exploration sector opens up new opportunities to further explore the capabilities of oil and gas exploration in deep water. With that being said, attention has been shifted to the optimization and production of drilling mud which is suitable for drilling operations. The selection drilling mud is often evaluated in compliance with the type of operations and suitability of geographical surroundings to avoid lost circulation of drilling fluid as well as to minimize costs throughout the well-construction process.

The usage of alternative base fluid apart from the conventional base fluid for drilling mud is considered in this project. Furthermore, the addition of nanoparticles

to further enhance the properties of drilling fluid is mainly focused in this project too. Not much studies has been conducted on the effects of addition of nanoparticles in palm oil based drilling fluid. However, comparisons of studies done on fluids with similar properties to drilling fluid is considered in this literature review.

2.2 Ball Milling

Ball milling which is known as mechanical alloying is the appropriate method to modify the morphology of multiwall carbon nanotubes (MWCNTs) due to the high pressure collisions between balls in the milling chamber. Inadequate milling intensity will result in little changes of morphology of MWCNT while excessive milling produces extreme damage to the shape of the carbon nanotubes (CNTs). Optimum ball milling intensity produces short and open-ended carbon nanotubes with less damage on its structure.

In a study carried out by Kukovecz, Kanyo, and Kiricsi (2005), 9.5cm × 11cm stainless steel drums and 110 stainless steel balls with mean diameter of 0.707cm was used to carried out the ball milling experiment with time duration from 1 to 200 hours. Results of the experiment proved that longer milling duration decreases nanotube lengths as well as reducing the entanglement of the tubes. At milling duration of 200 hours, they find out the structure of nanotubes are similar to those in the beginning of grinding with the rate of change becoming lower and quasi linear as the milling time increases.

A contrasting study carried out by Tucho et al. (2010), the ball milling experiment was done using planetary Fritsch P7 mill with 25 ml tempered steel vials and 10 mm diameter balls. At higher milling intensity at approximately 510 rpm, CNTs are successfully converted into carbon nanoparticles at 3 hours of total milling operations. Tucho et al. (2010) claimed that ball milling intensity produces much more significant changes to the morphology of the CNT as compared to the total milling time duration. At ball milling speed of 260 rpm with 1 to 10 hours of milling operations, no significant changes in structure of CNTs can be seen. They concluded their findings by suggesting moderate high speed at short milling duration to see remarkable changes in the structure at lower damage to the morphology structure of the CNTs.

2.3 Surface Tension

The dispersion of nanoparticles is largely influenced by the surface tension of the liquid. Surface tension is defined as the force acting over the surface of the liquid per length of the surface perpendicular to the force (Tanvir & Qiao, 2012). The surface tension of fluid is of particular interest for the microfluidics community such as pharmaceutical and paint coating applications. However, one of the focus in this study is to analyse appropriate range of surface tension for well-dispersed nanoparticles for oil-based nanofluids.

According to Li, Hong, Fang, Guo, and Lin (2010), metal nanoparticles have the tendency to form clusters which leads to precipitation of particles in the fluid phase(Li et al., 2010). This leads to obstruction of channels in heat transfer systems and reduction in thermal conductivities. Aggregates can be mainly divided into two types: aggregrate created by covalent bonds between primary particles and agglomerates defined as looser and more open structures that can be separated into primary component(Tinke, Govoreanu, Weuts, Vanhoutte, & Smaele, 2009). Agglomerates tend to hold each other through electrostatic forces, magnetic forces or interaction of flocculants in suspensions (Nguyen, Rouxel, & Vincent, 2014).

An experiment to investigate the surface tension of ethanol and n-decane nanofluid through the dispersion of Multi-Wall Carbon Nanotube (MWCNT) has been carried out by Tanvir and Qiao (2012). An ultrasonic disruptor with a series of 4-seconds-long pulses 4-seconds apart was generated to disperse the particles evenly to minimize the agglomeration effect. They concluded that surface tension of nanofluid is dependent on the particle's distribution and the addition of surfactant to nanofluid decreases its surface tension due to electrostatic repulsive force between particles (Tanvir & Qiao, 2012).

2.4 Nanoparticle Concentration

In a separate experiment, Nguyen et al. (2014) studies the dispersion of nanoparticles in various fluids ranging from organic solvents to polymer solutions through ultrasonification methods as well. Aluminium oxide (Al_2O_3) and zinc oxide (ZnO) nanoparticles with 13nm and 60 nm particle size respectively were used. They claimed that nanoparticle concentration could affect cluster size and viscosity of suspension as rheological behaviour is dependent on the solid loadings.

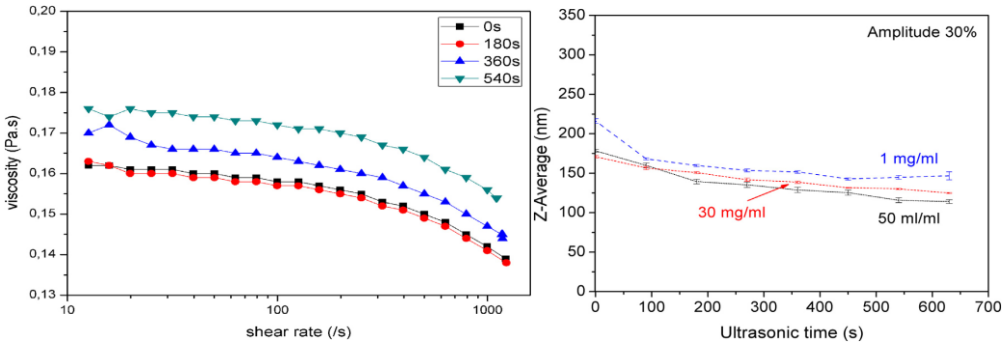

(a) (b)

Figure 1 : (a) Resulting viscosity at different ultrasonication time duration with increasing shear rate and (b) Cluster size of nano particles at increasing ultrasonication time.

The experiment was carried out at varying ultrasonification time duration and results shows dispersion of nanoparticles at high concentrations in solvent at increasing time shows decrement in Newtonian viscosity and cluster size of Al_2O_3 suspensions. They concluded that solid concentration have low effects on the formation of cluster size (Nguyen et al., 2014).

Li et al. (2010) carried out preparation of well-dispersed silver nanoparticles for non-polar oil-based nanofluids which can be of reference to the dispersion of functionalized graphene oxide (FGO) in this study project. The polarity of functional group ester is third to last least polar when compared to amide groups as most polar and alkane groups as the least polar. Li et al. (2010) had used surface-capped nanoparticles for their experiments and concluded that temperature plays no significant roles on the morphology of nanoparticles but have slight influence on size distribution. At higher pH level medium, the reaction medium remained clear to form a layer of even silver nanoparticles. Oleic acid is used to coat the surface of silver nanoparticles acts as a surfactant to prevent agglomeration.

2.5 Viscosity

In a research paper written by Ruan and Jacobi (2012), they cited that there are fluctuating results of significant changes of viscosity in nanofluids. Some researchers claimed that there are no changes while others noticed remarkable increment in terms of viscosity parameter. Besides that, nanofluid would result in a lower viscosity if better dispersion of nanoparticles are done. Their results also yield that viscosity of nanofluids will increase sharply before approaching the viscosity of the base fluid at

longer duration sonication time. The ideal maximum enhancement of viscosity was at 40 minutes mark of sonication time in the experiment.

A study conducted by Wang et al. (2012) disperses stable graphene nanoparticles at low loadings into ionic-liquid based nanofluids without the assistance of surfactants. A few properties studied by Wang et al. (2012) are also in alignment with the interest to produce alternative based drilling nanofluid. Such properties of interests include thermal conductivity and viscosity of the fluid as a function of temperature. 0.06%wt graphene loadings suspended in ionanofluid were found to have the highest thermal conductivity at higher temperature compared to the pure base fluid. Besides that, viscosity of the ionanofluid containing graphene nanoparticle suspension as a function of temperature is found to be lower at higher temperature compared to the base fluid.

With respect to the rheological properties, addition of MWCNT increases the mud's shear stress where it is linearly proportional to shear rate.

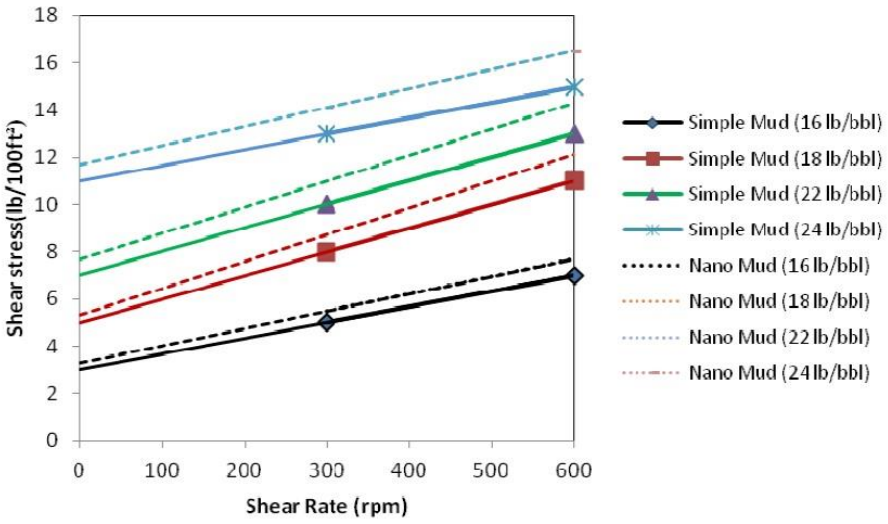

Figure 3 : Shear stress of water-based drilling fluid at increasing shear rate with different mud contents

Findings by Sedaghatzadeh et al. (2012) shows drilling mud containing the highest CNT loadings yields the highest shear stress. Sedaghatzadeh et al. (2012) concluded the findings that introduction of functionlized MWCNT supported previous studies done on the thermophysical properties and rheological enhancements.

2.6 Thermal Conductivity

In a separate study conducted by Sedaghatzadeh, Khodadadi, and Birgani (2012), an attempt to improve thermal and rheological properties of water-based drilling fluids using multiwall carbon nanotube (MWNCT) was carried out. MWCNT are hydrophobic in nature and is not readily dispersed in water. 69 wt% of nitric acid was refluxed with MWCNT to allow hydrophilic functional groups to be attached to the surface of the nanotubes. The measuring method used to conduct thermal conductivities of the nanofluid was through transient hotwire (THW) method. Due to the presence of bentonite in the base fluid, the precipitation of MWCNT occurs slowly and better stabilizes the nanofluid.

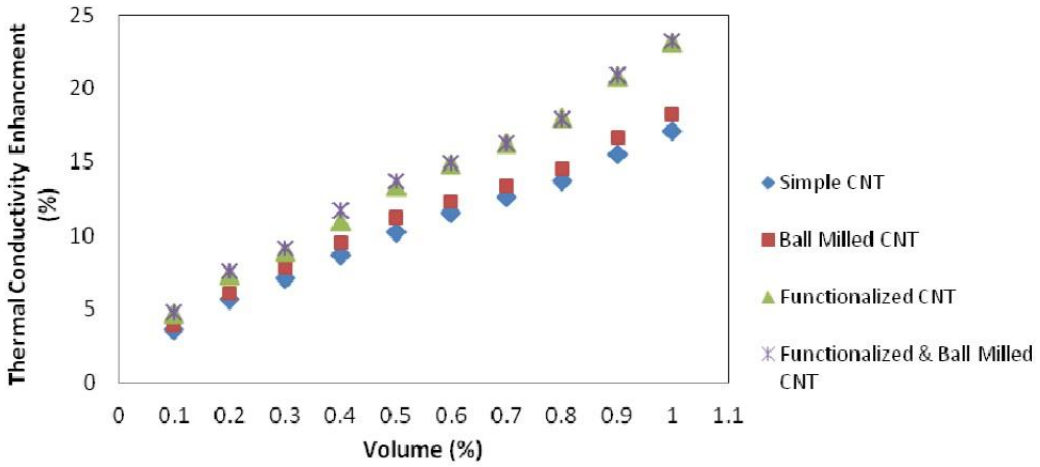

Figure 2 : Thermal conductivity experiment with increasing nanoparticle concentrations with different nanoparticle types

With this regard, functionalized and ball milled carbon nanotubes (CNT) were found to have the highest thermal conductivity enhancement compared to untreated CNT in various parameter conditions.

Ruan and Jacobi (2012) have carried out an experiment to determine the increment ratio between nanofluid thermal conductivity to base fluid thermal conductivity respectively against sonication time. Their results has reportedly shown a remarkable thermal conductivity increment by more than 10% in less than 100 minutes of total sonication time.

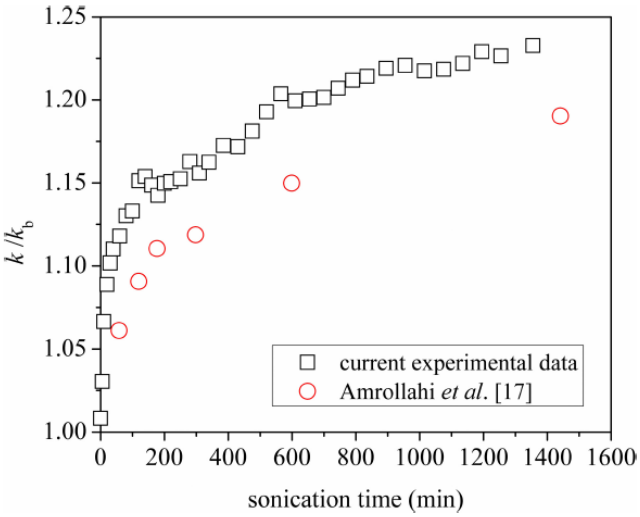

Figure 4: Thermal conductivity enhancement with respect to sonication time (min)

From the figure, the first hour of sonication gives a sharp thermal conductivity percentage increment before further increasing in a less inclined trend. They concluded that for maximum thermal conductivity enhancement, longer duration of sonication is applicable.

2.7 Ultrasonic Dispersion

There are two sonication dispersion methods involved mainly direct sonication and indirect sonication. The National Institute of Standards and Technology recommends direct sonication method over indirect sonication when used to disperse dry powder solids.

According to (Kun et al., 2013), they observed that the concentration of dispersed CNT is a function of the sonication energy applied instead of time duration of sonication process or the power output of the sonicator. Kun et al. observed that insufficient sonication energy will lead to inadequate dispersion of CNTs as well as bigger particle sizes. They also added that length and diameter of CNTs are a critical factor in sonication dispersion as longer tubes tend to entangle each other more easily due to its flexibility, resulting in agglomeration of the nanoparticles. However, Kun et al. uses the following correlation to identify the degree of CNT dispersion:

$$E = \frac{P \times t}{V} \qquad (1)$$

where P is the output power of sonicator, W; t is the total sonication time duration, s; and V is the total volume of liquid sonicated in the sonicator, mL. They concluded

that an optimal energy applied of 2250 $\pm$ 250J/mL yields higher stability of suspensions for at least 8 months.

2.8 Summary

The literature reviews mentioned spurs the intention to investigate the thermophysical properties and rheological properties of alternative base fluid for drilling mud as comparisons between different types of base fluids with the addition of nanoparticles are not conducted.Nanofluids containing suspended nanoparticles are known to have enhanced properties mainly significant increment in terms of thermal and rheological properties. Numerous studies have been carried out to determine the optimum parameters which affects such properties. Most studies yield back positive results.

CHAPTER 3

METHODOLOGY / PROJECT WORK

To study the effects of various base oils and various nanoparticle loadings, it is required to characterize and determine the sizes and compositions of the nanoparticles. Below is a general methodology that will be adapted for this project purposes.

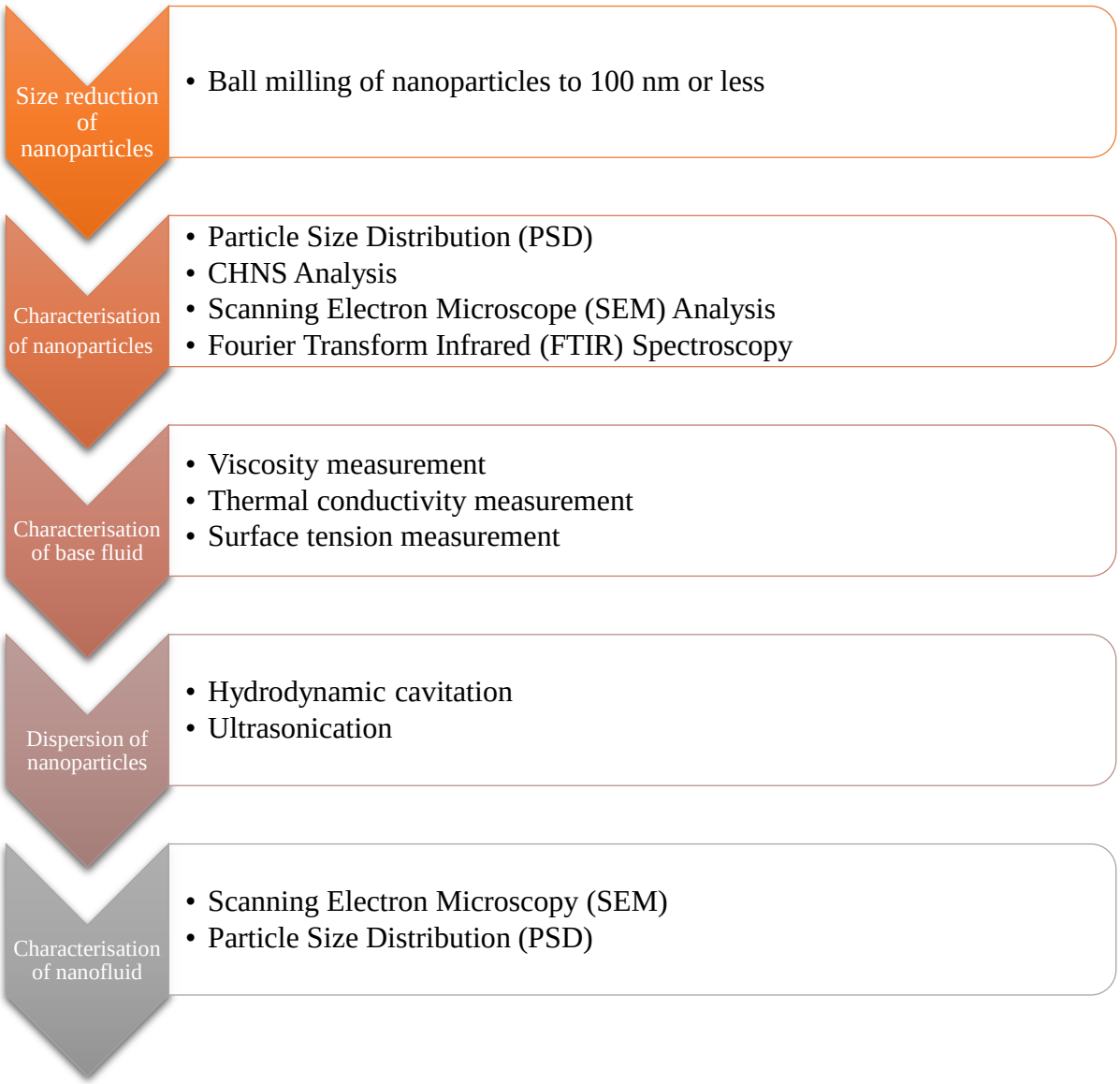

Figure 4 : Process flowchart for project methodology

3.1 Ball milling of carbon nanotubes

Figure 6: Planetary Mono Mill PULVERISETTE 6 *classic line*

Planetary Mono Mill PULVERISITTE 6 *classic line* is selected to ball mill carbon nanotubes into nanoparticles. The equipment selected contains a 250ml grinding bowl, with zirconium oxide material of construction. The diameter of grinding balls used are 5mm in diameter with zirconium oxide material of construction. The key parameters in this experiment followed the study conducted by Tucho et al. (2010).

Procedure:

1. 15g of carbon nanotube functionalised group –COOH Batch 1 was weighed and placed inside the grinding bowl. 25 grinding balls was placed on top of the samples.
2. ON SWITCH located at the back of the equipment was switched on.
3. The rubber sealer was placed in between the grinding bowl and the lid. The bowl's lid was ensure to tighten completely.
4. The grinding bowl was placed in the compartment provided. The safety lock was ensured to be locked properly before closing the equipment's main lid.
5. The rotary speed of 500rpm with a time duration of 3 hours, with 1 hour interval stop each hour was set.
6. After the sample was ball milled for 3 hours, the sample was stored in a dry container labelled Batch 1
7. The grinding bowl was thoroughly washed with soap water and air dried.
8. Step 1 to 7 was repeated with carbon nanotube functionalised group –COOH Batch 2.

3.2 Characterization of nanoparticles

1. Functionalized graphite nanofiber particles will be purchased from Platinum NanoChemSdn. Bhd.
2. Characterization and analysis of the purchased nanoparticles will be based on several parameters such as particle size distribution, surface topology and component composition.

3.2.1 Particle Size Distribution

Figure 7 : Malvern Mastersizer 2000 Particle Size Analyzer

It is desired to identify the size of the nanoparticle. The acceptable range of nanoparticle size is averagely at 100 nm or less. Due to high size distribution in metal nanoparticles, there exists a high tendency for the particles to agglomerate and form a colloid suspension due to high Van der Waals force between particles.

For the choice of equipment, Malvern Mastersizer 2000 Particle Size Analyzer is selected as it supports the size range of 20 nm to 2,000 μm. This range falls in the range of the requirement of nanoparticles to be 100 nm or less.

The equipment uses laser diffraction techniques to measure the particle sizes. This process is done by measuring the scattered light intensity as a laser beam passes through the dispersed particulate sample.

Procedure:

1. Before running the experiment, the refractive index and absorptivity factor of carbon nanotubes was determined.
2. Malvern Mastersizer 2000 was switched using the power switch located at the left lower corner of the equipment.
3. The values of both parameters was keyed into the software provided.
4. An approximate spoonful of carbon nanotubes functionalised group – COOH Batch 1 was taken with a dry spatula metal spoon/spade 150 mm.
5. The lid of optical bench of Malvern Mastersizer 2000 is opened and the sample is placed in the compartment. The lid was then closed.
6. The START button was clicked on the software to activate light scattering intensity to determine the size of the particles. The experiment was left to calculate the average particle size distribution
7. The measured sample was vacuumed into a waste storage compartment after particle size distribution experiment is completed.
8. The dry spatula metal spoon/spade 150mm was cleaned thoroughly with water and air dried to ensure no water particles adhered to the spatula.
9. Steps 3 to 7 were repeated with carbon nanotubes functionalised group – COOH Batch 2, ball-milled carbon nanoparticles functionalised group – COOH Batch 1 and ball-milled carbon nanoparticles functionalised group –COOH Batch 2.

3.2.2 Surface Topology

It is desired to obtain images of the nanoparticle surface topology. Such important characteristics include the layers of nanoparticles against one another and how specific topology and structures affect the dispersion of nanoparticles

For the choice of the equipment, Meiji MX-4300L Scanning Microscope is used to determine the surface topology of the nanoparticles. Electron images printout will be obtained and analysed to determine the orientation.

3.2.3 Component Composition

Figure 8: Perkin Elmer Transform Infrared Spectrometer (FTIR)

Fourier Transform Infrared (FTIR) spectroscopy is required to analyse the strength of absorption by nanoparticles as absorption is proportional to the concentration of a particular substance. The measurement through FTIR will give data on the chemical bonds and molecular structure of the nanoparticle.

Procedure:

1. The power switch located at the lower left side of the instrument was switched on.
2. The main tank valve on the nitrogen cylinder was opened. The flow-rate was pre-set to approximately 50ml/min.
3. The sample chamber was purged with nitrogen for 20 minutes before running a sample.
4. A small sample of ball-milled carbon nanoparticle functionalised group –COOH Batch 1 was inserted onto the sample holder in the sample chamber. The cover was closed and nitrogen purge was re-established while waiting for approximately 2 minutes.
5. The sample was scanned.
6. Properties of the result obtained on the computer desktop was pre-set and assisted by the laboratory's technician.
7. Step 2 to 6 are repeated with of ball-milled carbon nanoparticle functionalised group –COOH Batch 2.

3.3 Characterization of base fluids

1. Alternative base fluids will be purchased from Platinum NanoChemSdn. Bhd.
2. Rubber seed oil will be used to compare characteristics of the base fluids purchased.
3. Characterization and analysis of the purchased base fluids will be based on several parameters such as viscosity, thermal conductivity, and surface tension measurement

3.3.1 Density measurement

Figure 9: Anton Paar Density Meter 4500M

The density of the pure base fluids is measured using Anton Paar Density Meter 4500 M. The determination of density of pure base fluid is essential to calculate the amount of nanoparticle loadings required for dispersion applications.

Procedure:

1. The equipment was switched on and is left for 15 minutes to stabilise the temperature measurement pre-set at 20℃.
2. 1 mL of acetone is extracted using a 10 mL syringe. Acetone was injected into the density meter at the side inlet port.
3. 1 mL of base fluid (rubber seed oil) is extracted using a 10 mL syringe. Rubber seed oil was injected into the density meter at the side inlet port. It was ensured that no bubbles formation is found in the density meter.
4. The desired temperature measurement was set at 25℃. The equipment was left to stabilise until it reaches the set temperature.

5. START button was pressed and is left to measure the density at the set temperature.
6. The result of the measurement was recorded.
7. 1 mL of acetone was extracted using a 10 mL syringe and was injected into the side inlet port to dissolve rubber seed oil trapped in the density meter.
8. Water was extracted using a 10 mL syringe and was injected into the side inlet port to remove undissolved acetone.

3.3.2 Viscosity measurement

The equipment selected to measure the viscosity of the base fluid is Brookfield CAP 2000+ H Viscometer. The operating temperature limit for this equipment ranges from 5°C-75°C depending on the series model. The viscosity of the different base oil will be measured before and after the additions of nanoparticles for comparison purposes.

Procedure:

1. The equipment was switched on and is left for 5 minutes to stabilise the temperature measurement pre-set at 25℃.
2. The equipment was equipped with spindle 3 and is calibrated before running the experiment.
3. A dropper was used to extract the pure base fluid in the beaker. A few drops of the sample is placed on the plate of the viscometer.
4. The running time and holding time is set to 60s and 10s respectively. The handle of the viscometer was lowered until the spindle came in contact with the liquid surface.
5. To initiate the viscosity analysis, "RUN" button was pressed.
6. The viscosity results were recorded.
7. The shear rate and temperature of the measure liquid sample were adjusted to 100, 150 and 200 rpm from 25℃ to 45℃ with 5℃ increment respectively.
8. Steps 2 to steps 7 were repeated using 0.2wt%, 0.4wt%, 0.6wt%, 0.8wt% and 1.0wt% dispersed nanobased-fluid respectively.

3.33 Thermal conductivity measurement

The thermal conductivity analysis is carried out using P.A. Hilton Thermal Conductivity of Liquids and Gases Unit H471. A heater is contained within the vessel where the space around the unit filled with the sample fluid analysed. A water jacket surrounds the outer space of the sample fluid. The thermal conductivity measurement is done by measuring the temperature of two thermocouple points across cross sectional area of the vessel located at the space of sample fluid and wall of water jacket respectively. The equipment's maximum voltage deliverance limit is 40 V and 60 V for gaseous samples and liquid samples respectively.

The radial clearance of the equipment is 0.3 mm with cross-sectional heat transfer area of 0.0134m^2. The resistance of the heater is 55Ω. The voltage delivered ranges from 0 V to 60 V for liquid samples. The thermal conductivity of the sample fluid can be calculated from the equation below:

$$\text{Thermal conductivity, } k = \frac{Q\Delta T}{A\Delta T} \qquad (2)$$

The heat input by the equipment can be calculated from the equation below:

$$\text{Heat Input, } Q = \frac{V^2}{R} \qquad (3)$$

However, incidental heat transfer, Q_I, must also be accounted in the calculation. Incidental heat transfer includes heat transferred through walls of the vessel and bolts. The incidental heat transfer can be estimated from the figure below:

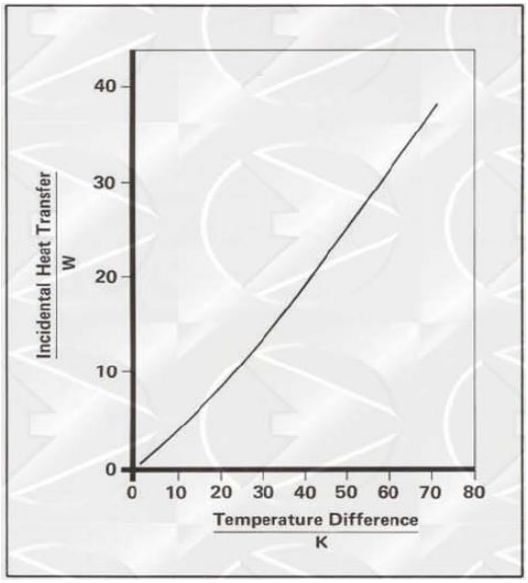

Figure 10: Incidental heat transfer, W with respect to temperature difference

The incidental heat transfer must be deducted from the total heat input to obtain the true value of heat conducted through the sample fluid.

$$\text{Heat conducted, } Q_C = Q - Q_I \qquad (4)$$

The schematic drawing of the equipment is illustrated in the figure below:

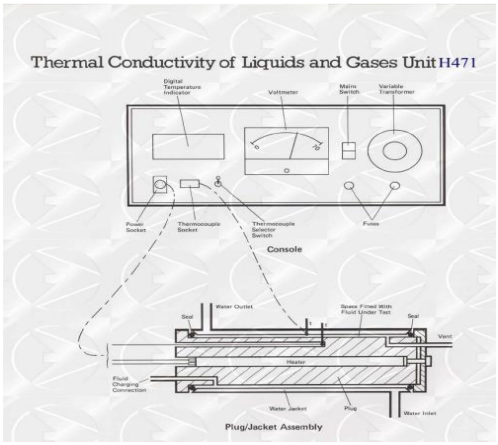

Figure 11: P.A. Hilton Thermal Conductivity of Liquids and Gases Unit H471

Procedure:

1. Water was flowed into the water jacket cooler at constant flow rate.
2. H471 unit equipment was switched on and it was made sure that the knob was at point 0.
3. Water was flowed to the side inlet of the vessel to remove any contaminants within the vessel.

4. Air was flowed at constant flow rate to air dry the wetted pathway within the vessel.
5. 10 mL of pure base fluid was extracted using a syringe and was injected into the side inlet of the vessel.
6. The knob was turned from 0 to the point where the voltage delivered by the equipment is at 60V.
7. The temperature was left to stabilise before temperature points at the heater and wall of water jacket was taken.
8. The thermal conductivity of the fluid was calculated based on Equation (2).
9. Water was flowed into the side inlet to flush out the residual of cabon nanoparticles that may be suspended within the pathway space.
10. Air was flowed into the vessel to dry air the wetted pathway.
11. The experiment was repeated from steps 5 to steps 10 using 0.2wt%, 0.4wt%, 0.6wt%, 0.8wt% and 1.0wt% nanoparticle loadings dispersed into the base fluid.

3.4 Dispersion of nanoparticles

1. Refined functionalized nanoparticles will be disperse into alternative base fluids through hydrodynamic cavitation and ultrasonication.
2. There will be three (3) comparisons between each experiments mainly data comparisons between the experiments as follows:
    a. Hydrodynamic cavitation of nanofluid only
    b. Ultrasonication of nanofluid only
    c. Hydrodynamic cavitation followed by ultrasonication of nanofluid

3.4.1 Ultrasonication

Ultrasonication is the irradiation of liquid sample with ultrasonic waves which results in a series of propagation of waves in high and low pressure cycles. Nanoparticles will be added into a base fluid and undergo ultrasonication, where high-intensity sonic waves creates small vacuum voids

in the liquid and is collapsed violently through compression creating high local temperatures within the fluid itself. Therefore, ultrasonication requires to be carried out in a water bath, where the resulting temperature of the nanofluid remains constant throughout.

There will be multiple experiments to be conducted where data comparisons will be made. Alternative base fluids at constant nanoparticles loading will be carried out for ultrasonicaon to study the effects of different base fluids on the suspension of the nanoparticles in base fluid. The manipulative variable in this experiment would be the type of base fluids used and the pressure difference across the equipment. The resulting variable will be the time duration of suspension of nanoparticles in the base fluid.

The study of nanoparticles loadings effect will also be investigated by varying the weightage loading of the nanoparticles into different base oil through ultrasonication. The manipulative variable in this experiment is the variation in nanoparticle loadings into base fluid. The resulting variable of this experiment will be the thermal conductivity and rheological properties of the nanofluid.

3.5 Characterization of nanofluid

1. The resulting produced nanofluid by batches between different base fluids and different nanoparticle loadings will be analysed to determine the nanofluid's individual characteristics.
2. PSD and SEM analysis is required to analyse the size distribution and orientation of nanoparticles in the base fluid.
3. Thermal conductivity and rheological properties of the base nanofluid will be analysed using Brookfield CAP 2000+ H Viscometer and Thermal Conductivity Analyzer. The data obtained on the physical properties of the base nanofluid will be compared to the pure base fluid.

3.6 Gantt Chart

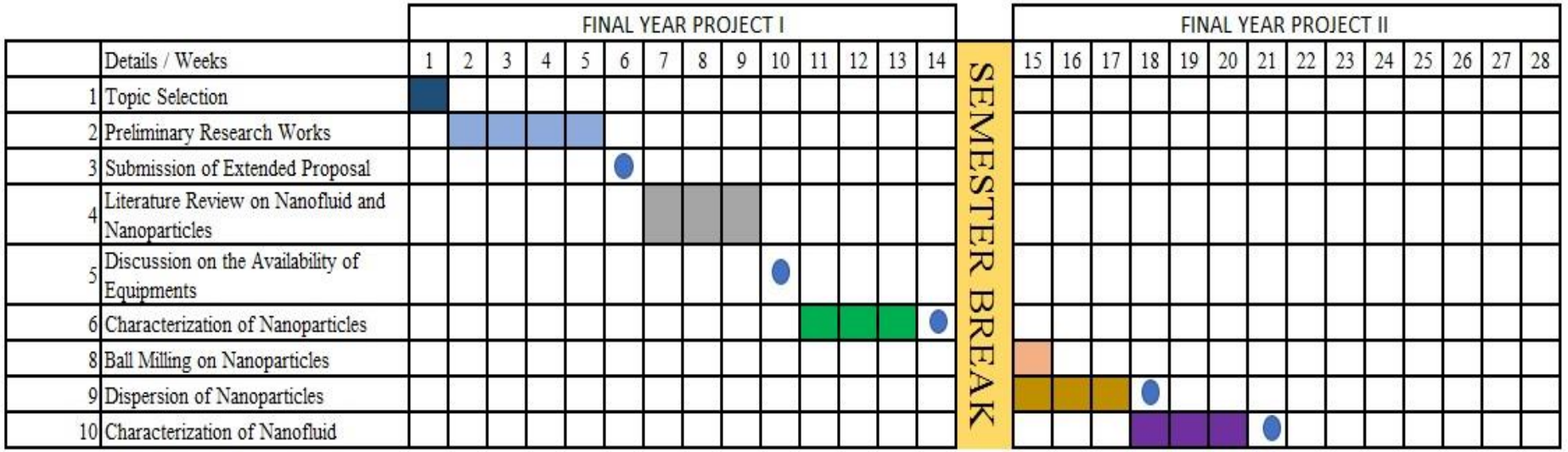

Figure 12: Gantt Chart for Final Year Project experimentations

3.7 Project / Key Milestones

Week 6 – Submission of Extended Proposal

Week 10 – Completion of major equipment identification

Week 14 – Completion of characterization of nanoparticles experimentations

Week 18 – Completion of nanoparticles dispersion experimentations

Week 21 – Completion of nanofluid characterization experimentations

CHAPTER 4

RESULTS AND DISCUSSION

4.1Particle Size Distribution (PSD)

The figures below shows the average particle size distribution of carbon nanotubes functionalised group –COOH Batch 1 and Batch 2, and ball-milled carbon nanoparticles functionalised group –COOH Batch 1 and Batch 2.

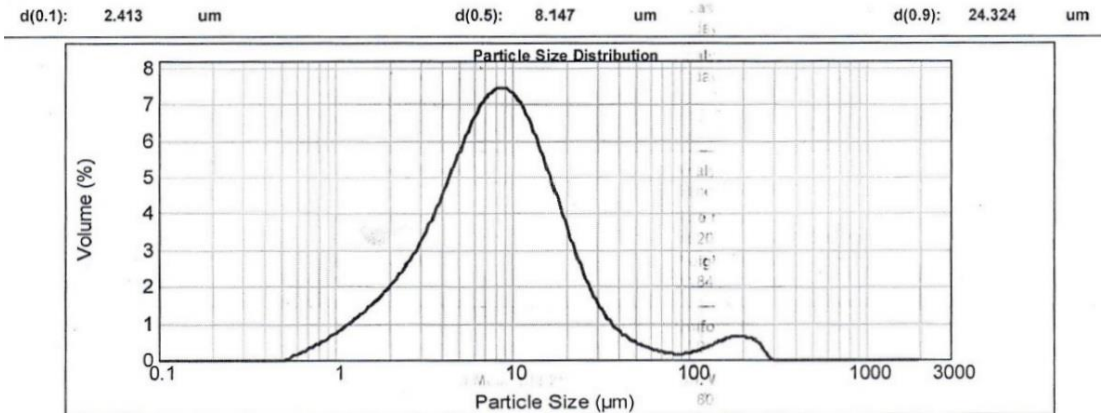

Figure 13: Particle size distribution of carbon nanotubes (CNTs) functionalised group –COOH Batch 1

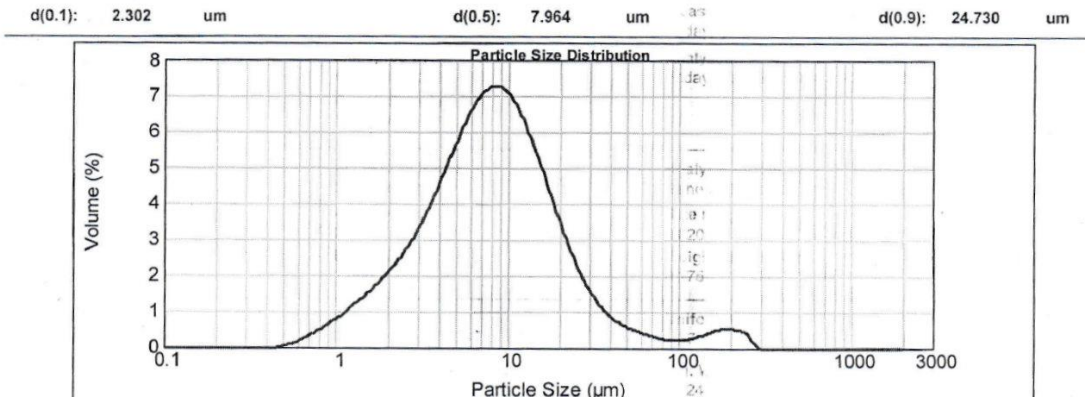

Figure 14:: Particle size distribution of carbon nanotubes (CNTs) functionalised group –COOH Batch 2

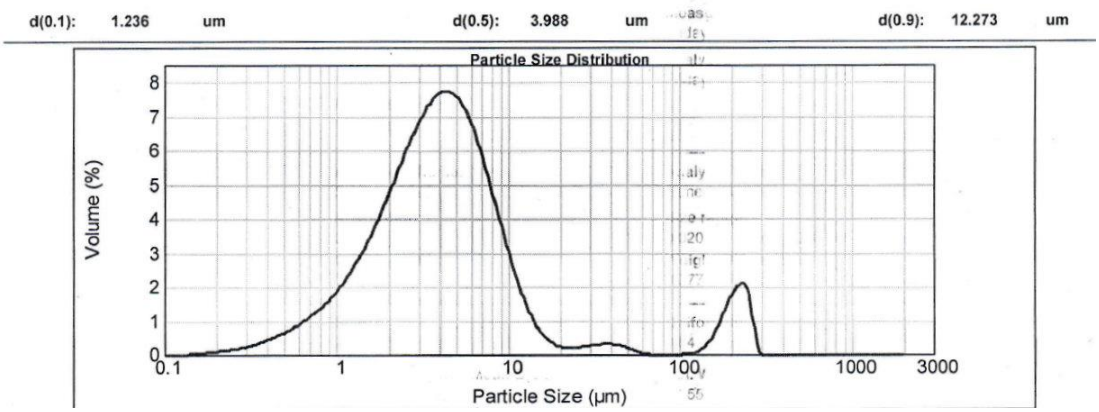

Figure 15: Particle size distribution of ball-milled carbon nanoparticles functionalised group –COOH Batch 1

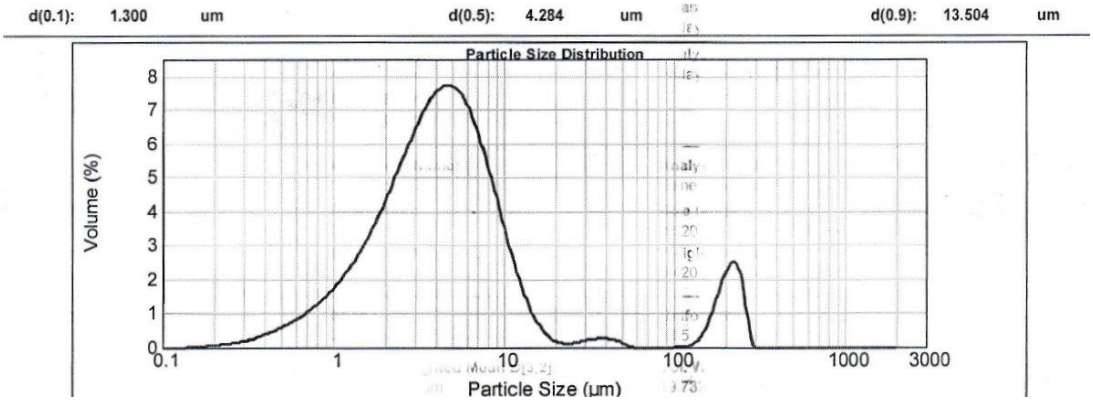

Figure 16:: Particle size distribution of ball-milled carbon nanoparticles functionalised group –COOH Batch 2

The table below summarizes and compares the findings of the results obtained for particle size distribution of the carbon nanotubes before and after ball milling.

Table 1 : Summary and comparisons between findings of particle size distribution of carbon nanotubes

Type	**Before Ball Milling**		**After Ball Milling**	
	Batch 1	**Batch 2**	**Batch 1**	**Batch 2**
Particle Size Distribution				
d(0.1)	2.413μm	2.302 μm	1.236μm	1.300μm
d(0.9)	24.324μm	24.730μm	12.273μm	13.504μm
Comparisons	**Batch 1**			
	d(0.1)	4.6%		
	d(0.9)	1.6%		
	Batch 2			
	d(0.1)	4.9%		
	d(0.9)	9.1%		
	Overall			
	Batch 1 - d(0.1)	48.8%		
	Batch 2 - d(0.9)	45.4%		

Figures 11 – 14 depicts the average particle size distribution of the carbon nanotubes and carbon nanoparticles which are before and after ball-milling respectively.

Figure 11 and Figure 12 displays the results of CNTs before ball-milling of Batch 1 and Batch 2 respectively. In Figure 11, 10% of the total population measured is averagely 2.413 μm and 90% of the total population giving a measurement of 24.324μm averagely. Similarly in Figure 12, 10% of the total distribution yields an average of 2.302 μm and 90% of the total population gives 24.730μm averagely in readings. The size differences between both batches shows a margin difference of 4.6% at the lower quartile while at the higher quartile, the differences appear relatively similar with only 1.6% length differences.

Figure 13 and 14 displays the results of CNTs after ball-milling of Batch 1 and Batch 2 respectively. In Figure 13, 10% of the total population gives a reduction in measurement length at 1.236 μm while 90% of the total population also gives a

reduction in length at 12.273μm. In a similar trend, Figure 14 shows 10% of the total population at a reduced length of 1.300μm and 90% at 13.504μm.The differences between both batches after being ball milled shows alike comparisons with 4.9% differences in length at 10% of the total distribution and slightly marginal differences of 9.1% at 90% of the total distribution.

Overall, the comparison in size of both Batch 1 and 2 before and after ball milling shows a total reduction in size by 48.8% and 45.4% respectively, with more or less reduction size of half of the length of the carbon nanotubes.

For the preparation of ultrasonic dispersion of nanoparticles, the pre-requisite for a good dispersion and a stable suspension requires nanoparticles at 200 nm or shorter. This is further supported by literature reviews of previous experimental works which dispersed similar sizes of nanoparticles. In this experiment, the ball-milled samples does not fully fit the requirement as 90% of the total population distribution yields sizes larger than 200 nm. The nature of the size of the carbon nanoparticles may give rise to the tendency to agglomerate or tangled each other when disperse under ultrasonic dispersion.

Ball milling of carbon nanotubes experiment is carried in accordance to the study conducted by Tucho et al. (2010), where key parameters involved in this experiment are the speed factor and time duration for the ball milling process. 500 rpm and 3 hours of total duration of intense ball milling experiment was carried out. However, from previous experience by conducted by UTP's postgraduates, they have found out that traces of zirconium oxide can be found in their sample analysis if the samples were ball milled for more than an hour. This may be due to the high intensity of impact between the grinding balls and the walls of the grinding bowls, which scrapes off trace amounts of zirconium oxide into the samples.

Therefore, to prevent any contamination of zirconium oxide into the carbon nanoparticle samples, at every hour of ball milling operations, there will be an hour of interval stoppage before the next hour of ball milling. At the same time, this could also prevent deformation of the morphology of the carbon nanoparticles due to high temperature as a result of extreme intensity from the collision of the grinding bowls. However, this factor that may very well attribute to the insufficient size of the nanoparticles at nano level.

The collision intensity of the grinding balls might not build up sufficiently over the total 3 hours of ball milling duration as suggested by Tucho et al. (2010) as there is an interval between each hour of ball milling operations.

4.2 Fourier Transform Infrared (FTIR) Spectrometry Analysis

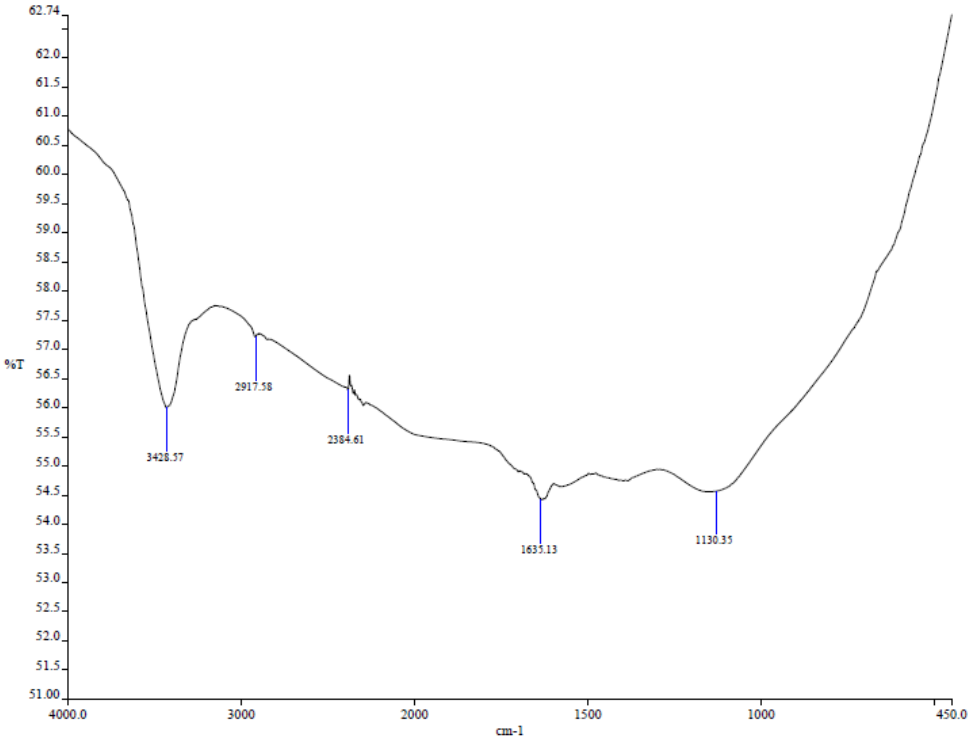

Figure 17: IR spectroscopy graph of ball milled carbon nanoparticle functionalised group –COOH Batch 1

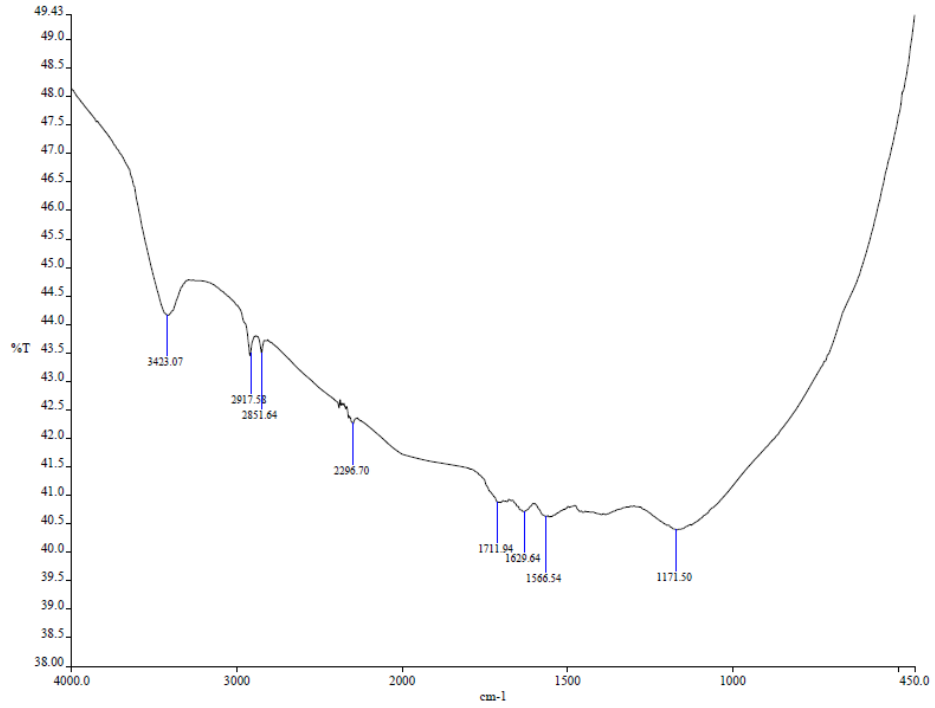

Figure 18: IR spectroscopy graph of ball milled carbon nanoparticle functionalised group –COOH Batch 2

Figure 15 and Figure 16 above show Fourier Transform Infrared Spectroscopy (FTIR) analysis result of ball milled carbon nanoparticles functionalised group –COOH Batch 1 and Batch 2. A table of characteristic IR absorptions (refer to Appendix) is used to determine the presence of the bonds and functional group in the samples.

In Figure 15, there is a broad peak with wavelength 3428.7 cm^{-1} which shows presence of O-H stretch bond or H-bonds which shows the presence of possible alcohol or phenol groups. A small peak can be seen at wavelength 2917.58 cm^{-1} showing the presence of O-H stretches with carboxylic acids as its main functional group. The analysis shows medium peak at 1635.13 cm^{-1} containing carboxylic acid functional group as well. Another smaller broader peak at 1130.35cm^{-1} also show C-O stretch bonds containing carboxylic acid group.

Similarly in Figure 16, a medium peak can be found at 3423.07 cm^{-1} identified having O-H stretch bonds or H bonds with functional group of either alcohols or phenols. As compared to Batch 1, an extra peak at frequency of 2851.64 cm^{-1} falls under the category of alkanes with C-H bonds. At frequency 1711.94 cm^{-1} and 1629.64 cm^{-1}, the peak shows the presence of carboxylic acid functional groups in the sample.

However, an extra peak at 1566.54 cm^{-1} C-C bonds with ring formations with possible aromatic functional groups present within in the sample.

4.3 Density

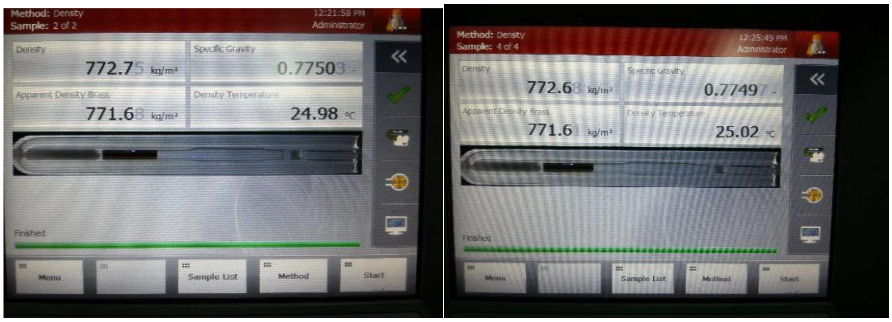

(a) (b)

Figure 19: (a) Density of 771.68 kg/m^3 at 25℃. (b) Density of 771.61 kg/m^3 at 25.02℃

Acetone is used as a solvent to dissolve the trapped liquid found within U-tube within the density meter. It also absorbs remaining water trapped as well, making it an ideal solvent for elimination of samples and water.

From the results obtained, at temperature of 25℃ the average density of pure base fluid is taken to be 910 kg/m^3.

$$\text{Average density, } \rho_{\text{average}} = \frac{771.68\frac{\text{kg}}{\text{m3}} + 771.61\frac{\text{kg}}{\text{m3}}}{2}$$

$$= 771.65 \text{ kg/m}^3$$

Determination of density of pure base fluid is essential to calculate the amount of nanoparticle loadings to be dispersed. The volume of pure base fluid to be dispersed required for each experiment is 100mL. The density of 771.65 kg/m^3 can be converted to 0.772 g/mL. The weightage loadings required for carbon nanoparticles to be dispersed can be calculated by multiplying the percent weightage loadings at 100 mL volume each.

Table 2: Carbon nanoparticle mass with respect to nanoparticle loadings, wt%

Nanoparticle loadings, wt%	Mass (g)
0.2	0.155
0.4	0.309
0.6	0.463
0.8	0.617
1.0	0.771

The above table summarises the amount of carbon nanoparticle mass required to be dispersed at the desired loadings.

4.4 Thermal Conductivity Analysis

The nanoparticle loadings carried out ranges from 0.2 wt% to 1 wt%. From literature review, it was predicted that there will be greater thermal conductivity enhancements with increasing nanoparticle loadings dispersed into base fluid. The figure below shows the relative thermal conductivity enhancements with respect to the nanoparticle loadings, in wt%.

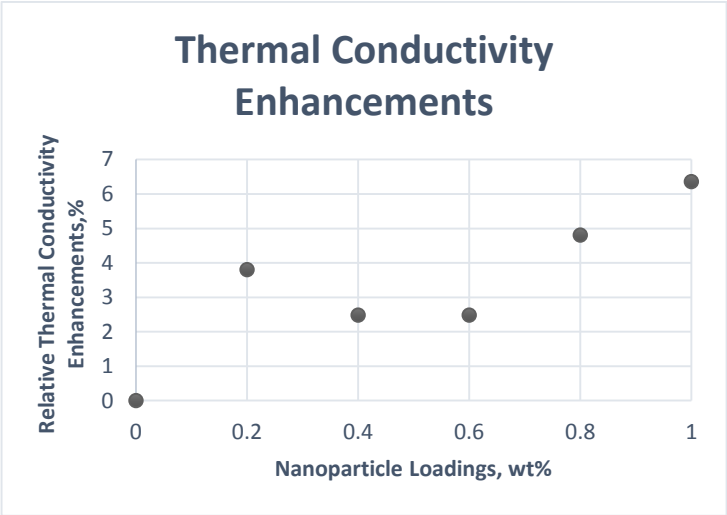

Figure 20: Relative thermal conductivity enhancement with respect to nanoparticle loadings

From the figure above, a fluctuating trend can be seen when nanoparticle loadings are increased from 0.2wt% to 0.6wt%. This inconsistent behaviour of the

fluid can be contributed to the inconsistency of water flowing around the jacketed area. Higher water flow rate cools down shell side's temperature, resulting in higher difference of temperature gradient between both thermocouple points.

Due to the larger size of carbon nanoparticles, the Van der Waals interactions between particles are greater. This results in greater attractions between particles, causing possible agglomerations and forms cluster sizes. Formation of cluster sizes results in clogging of heat transfer channel systems and lower thermal conductivity of the fluid. (Dan, Biyuan, Wenjun, Yongsheng, & Ruisen, 2010)The formation of cluster sizes or agglomerations also increases the rate of settling of carbon nanoparticles, giving a poor suspension of the nanoparticles in the base fluid.

4.5 Nanoparticle Suspension

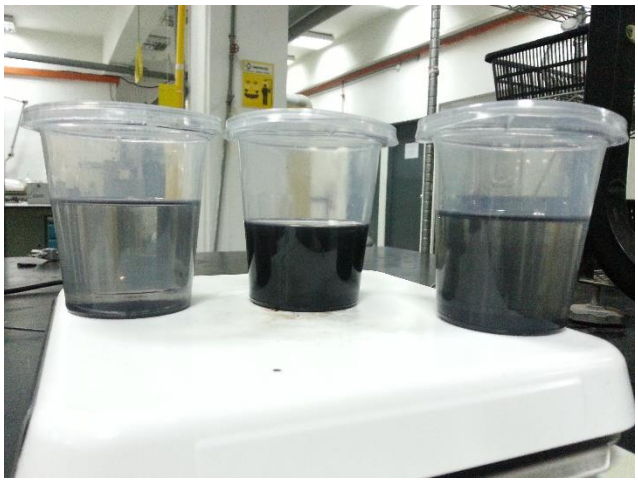

Figure 21: Comparison of nanoparticle suspensions between different post-sonicated base fluids

In this research study, the suspended carbon nanoparticles within the fluid are unable to suspend itself as long as what was done by literature reviews. The maximum duration for carbon nanoparticles to suspend itself before settling down completely was approximately two days with 0.4 wt% nanoparticle loadings.

This undesired short suspension duration can be attributed to the larger carbon nanoparticle sizes and the inadequate sonication energy delivered during ultrasonic dispersion. The carbon nanoparticles agglomerated and formed cluster sizes and settled down at a higher rate.

4.6 Viscosity

Below shows the viscosity of pure base fluids and nano-based fluids at different nanoparticle loadings at different shear rate, rpm, from 25℃ to 45℃.

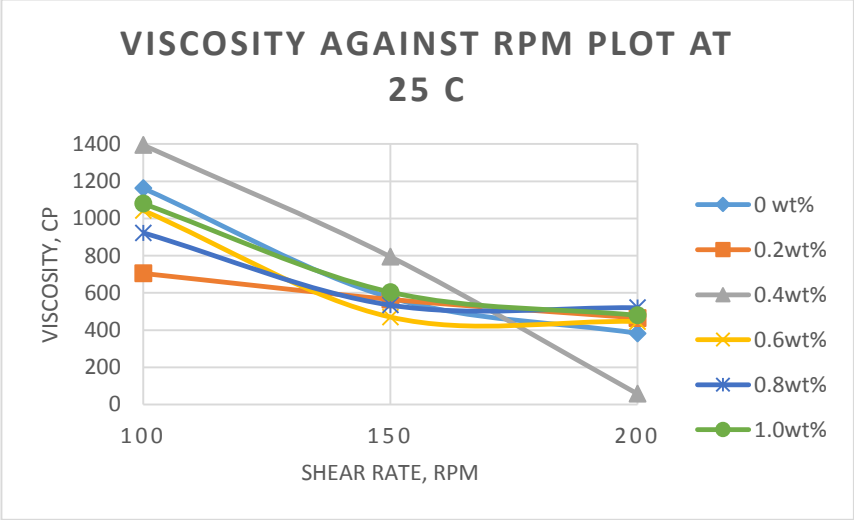

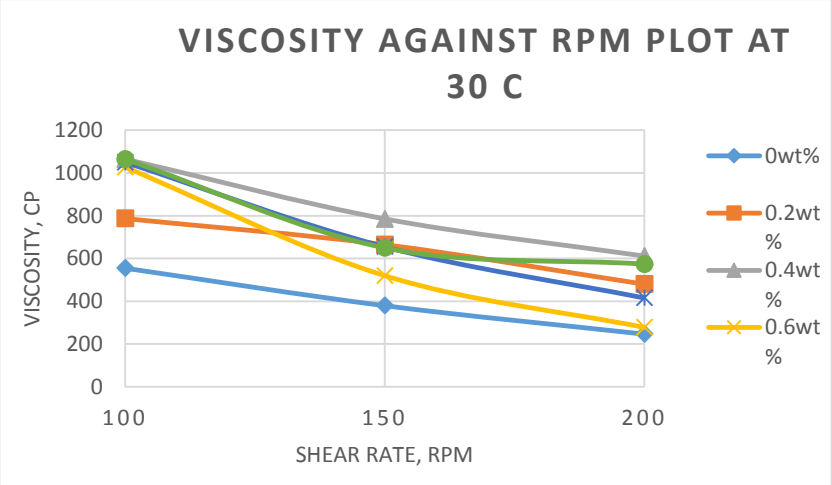

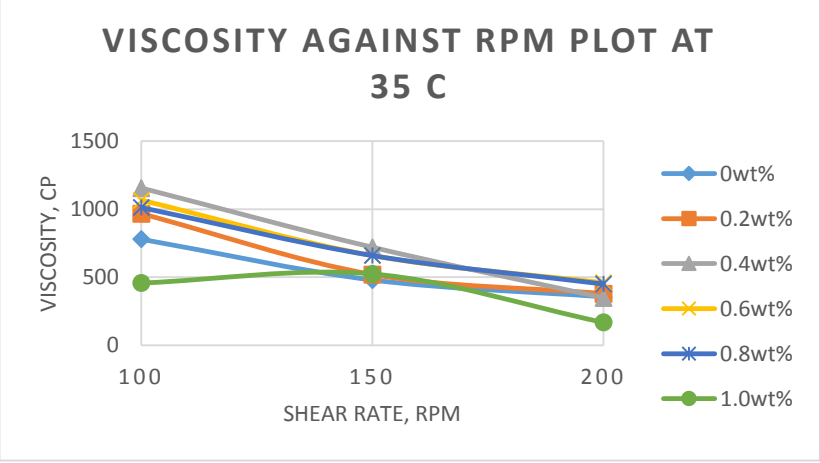

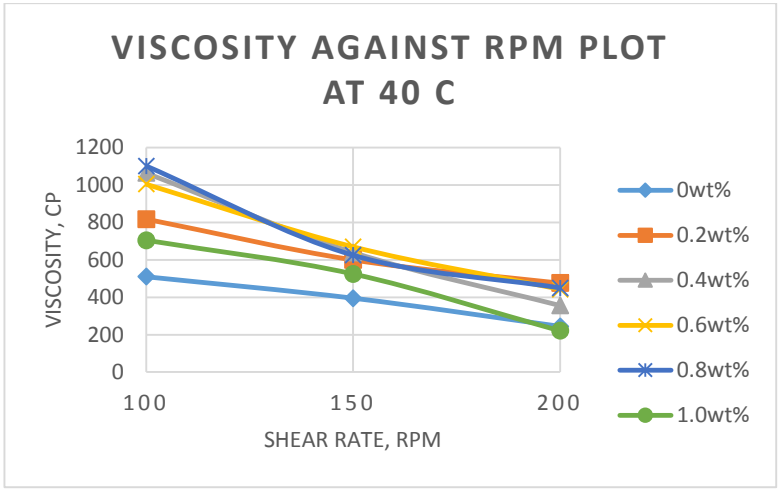

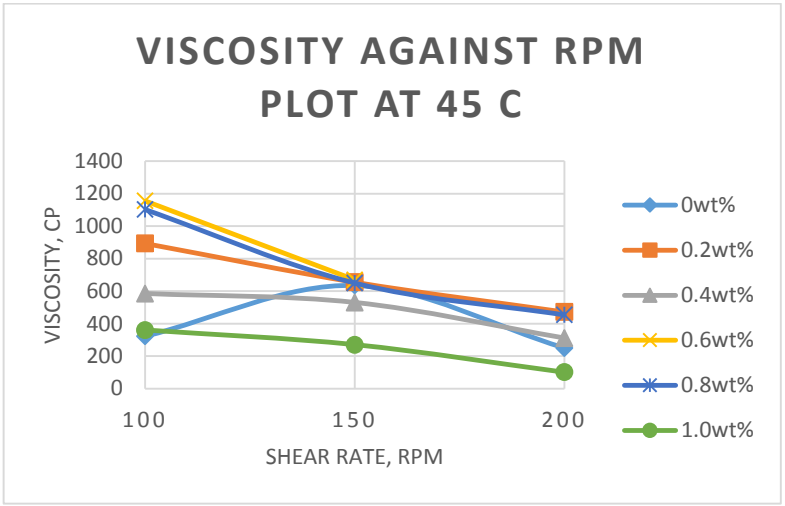

Figure 22: Viscosity of nano-based fluids with alternate nanoparticle loadings at different shear rate at temperature range from 25℃ to 45℃

From the plots above, a general trend can be observed for most of nano-based fluids where at higher shear rate, the viscosity tends to decrease exponentially. It can be generalised that the viscosity of each nano-based fluids are approximately similar to the one another. According to Ruan and Jacobi (2012), they cited in their study that different researchers concluded their findings pertaining to viscosity with fluctuating results as well. An accurate measurement of one liquid sample is hard to be defined.

However, fluctuations can be seen from the plots above. At initial shear rate of 100rpm, the viscosity at different nanoparticle loadings with temperature ranging from 25℃ to 45℃ fluctuates at each plots. The experiment was carried out using a dropper to extract the sample from the beaker to be place on the plate. The extraction process with the dropper might extract higher nanoparticles concentrations at certain points of depth and level in the beaker, thus giving higher viscosity results compared to other

nanobased-fluids. This can be attributed to the inadequate even dispersion of carbon nanoparticles within the base fluid. The uneven dispersion leads to agglomerations and subsequently form cluster sizes. Formation of cluster sizes increases the viscosity of the nanobased-fluid as high concentration of nanoparticles are centred within the extracted sample.

However, it can be deduced that at higher shear rates, the viscosity of nano-based fluids with different nanoparticle loadings is converging closer towards the viscosity of the pure base fluid. This is an important point to be taken note of as low viscosity is desired during drilling operations to reduce unwanted excess energy required in drilling processes.

4.7 Summary

From the results obtained, carbon nanoparticles are not ball-milled to the required sizes, which are at 200 nm or less. The current ball-milled carbon nanoparticles are at averagely 1,000 nm. Due to the larger size of the nanoparticles, the suspension and thermal conductivity of the nano-based fluid are not as hypothesized. It can be concluded that at 1wt%, it gives the highest thermal conductivity enhancement with a total enhancement of 6%. However, at various nanoparticle loadings, the viscosity of nano-based fluids can be seen approaching the viscosity of base fluid at higher shear rate regardless of operating temperature.

CHAPTER 5

CONCLUSION AND RECOMMENDATION

5.1 Conclusion

It can be concluded that from previous literature reviews and studies carried out on the enhancement of the fluid's properties can be further improved with the addition of nanoparticles. Such improvements include the thermal conductivity and the rheological properties of the fluid which extends beyond the limit of a pure base fluid.

In conclusion, at 1wt% of nanoparticle loading gives the highest thermal conductivity enhancement with a total enhancement of 6%. However, at various nanoparticle loadings, the viscosity of nano-based fluids can be seen approaching the viscosity of base fluid at higher shear rate regardless of operating temperature.

5.2 Recommendation

Use of surfactants to suspend nanoparticles within the base fluid is recommended in future study. Study shows that usage of surfactants gives longer suspension duration of nanoparticles, resulting in better dispersion of the nanoparticles.

REFERENCES

Dan, Li, Biyuan, Hong, Wenjun, Fang, Yongsheng, Guo, & Ruisen, Lin. (2010). Preparation of Well-Dispersed Silver Nanoparticles for Oil-Based Nanofluids. *Industrial & Engineering Chemistry Research, 49*, 1697-1702.

Functions of a Drilling Fluid (2012). Retrieved March 3, 2014, from http://petrowiki.spe.org/Functions_of_drilling_fluid

Hashim, Uda, Nadia, Elly, & Salleh, Shahrir. (2009). Nanotechnology development status in Malaysia: industrialization strategy and practices. *International Journal of Nanoelectronics and Materials, 2*(No. 1), 119 - 134.

Kukovecz, Akos, Kanyo, Timea, & Kiricsi, Imre. (2005). Long-time low-impact ball milling of milti-wall carbon nanotubes. *Carbon, 43*, 994-1000.

Kun, Yang, ZiLi, Yi, QingFeng, Jing, RenLiang, Yue, Wei, Jiang, & DaoHui, Lin. (2013). Sonication-assisted dispersion of carbon nanotubes in aqueuous solutions of anionic surfactant SDBS: The role of sonication energy. *Chinese Science Bulletin, Vol. 58*(17), 2082-2090.

Li, Dan, Hong, Biyuan, Fang, Wenjun, Guo, Yongsheng, & Lin, Ruisen. (2010). Preparation of Well-Dispersed Silver Nanoparticles for Oil-Based Nanofluids. *Ind. Eng. Chem. Res., 49*(4), 169 - 1702.

Nguyen, Van Son, Rouxel, Didier, & Vincent, Brice. (2014). Dispersion of nanoparticles: From organic solvents to polymer solutions. *Ultrasonics Sonochemistry, 21*, 149 - 153.

Ruan, Binglu, & Jacobi, Anthony M. (2012). Ultrasonication effects on thermal and rheological properties of carbon nanotube suspensions. *Nanoscale Research Letters, 7*(127).

Sedaghatzadeh, M., Khodadadi, A. A., & Birgani, M.R. Tahmasebi. (2012). An Improvement in Thermal and Rheological Properties of Water-based Drilling Fluids Using Multiwall Carbon Nanotube (MWCNT). *Iranian Journal of Oil and Gas Science and Technology, 1*(No. 1), 55-65.

Tanvir, Saad, & Qiao, Li. (2012). Surface tension of Nanofluid-type fuels containing suspended materials. *SpringerOpen*(7), 226.

Tinke, A.P., Govoreanu, R., Weuts, I., Vanhoutte, K., & Smaele, D. De. (2009). A review of underlying fundamentals in a wet dispersion size analysis of powders. *Powder Technology*, *196*, 102 - 114.

Tucho, W.M., Mauroy, H., Walmsley, J.C., Deledda, S., Holmestad, R., & Hauback, B.C. (2010). The effects of ball milling intensity on morphology of multiwall carbon nanotubes *Scripta Materialia*, *63*, 637 - 640.

Wang, Fuxian, Han, Lijuan, Zhang, Zhengguo, Fang, Xiaoming, Shi, Jingjing, & Ma, Wenshi. (2012). Surfactant-free ionic liquid-based nanofluids with remarkable thermal conductivity enhancement at very low loading of graphene. *SpringerOpen*, *7*, 314.

Wellbore.). from http://www.investopedia.com/terms/w/wellbore.asp

Wong, Kaufui V., & Leon, Omar de. (2009). Application of Nanofluids: Current and Future. *Advances in Mechanical Engineering*, *2010*, 11.

APPENDIX

Experimental

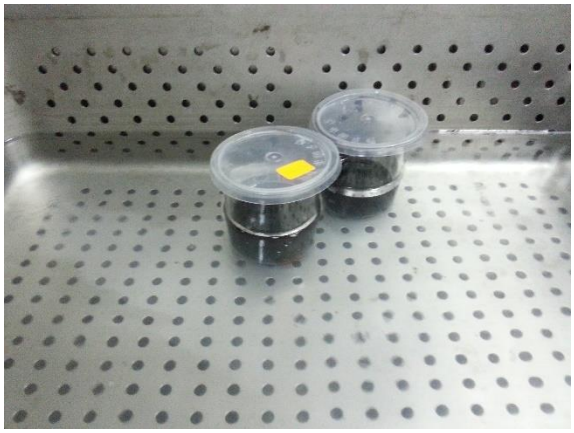

Figure 22: Ultrasonic bath dispersion of carbon nanoparticles

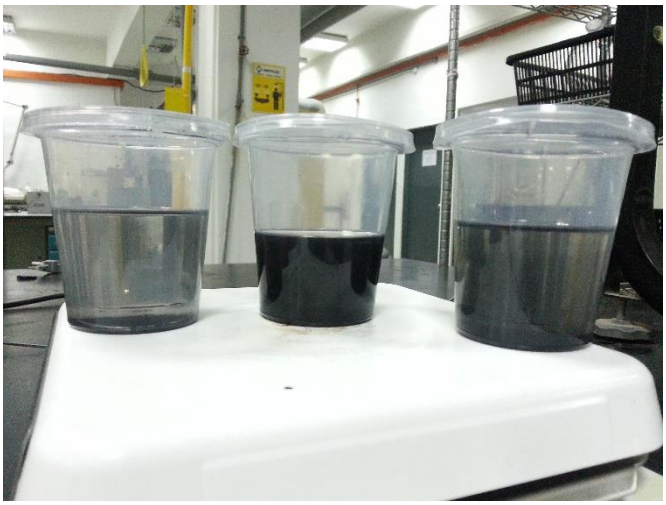

Figure 23: Comparisons between sonicated carbon nanoparticles (middle) in base fluid and post-sonicated carbon nanoparticles in base fluids

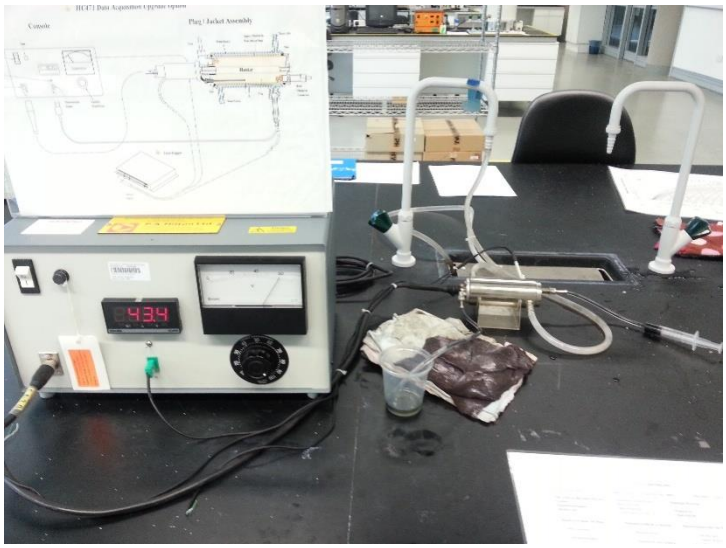

Figure 24: Thermal conductivity of base fluids and nano-base fluids with unit H471

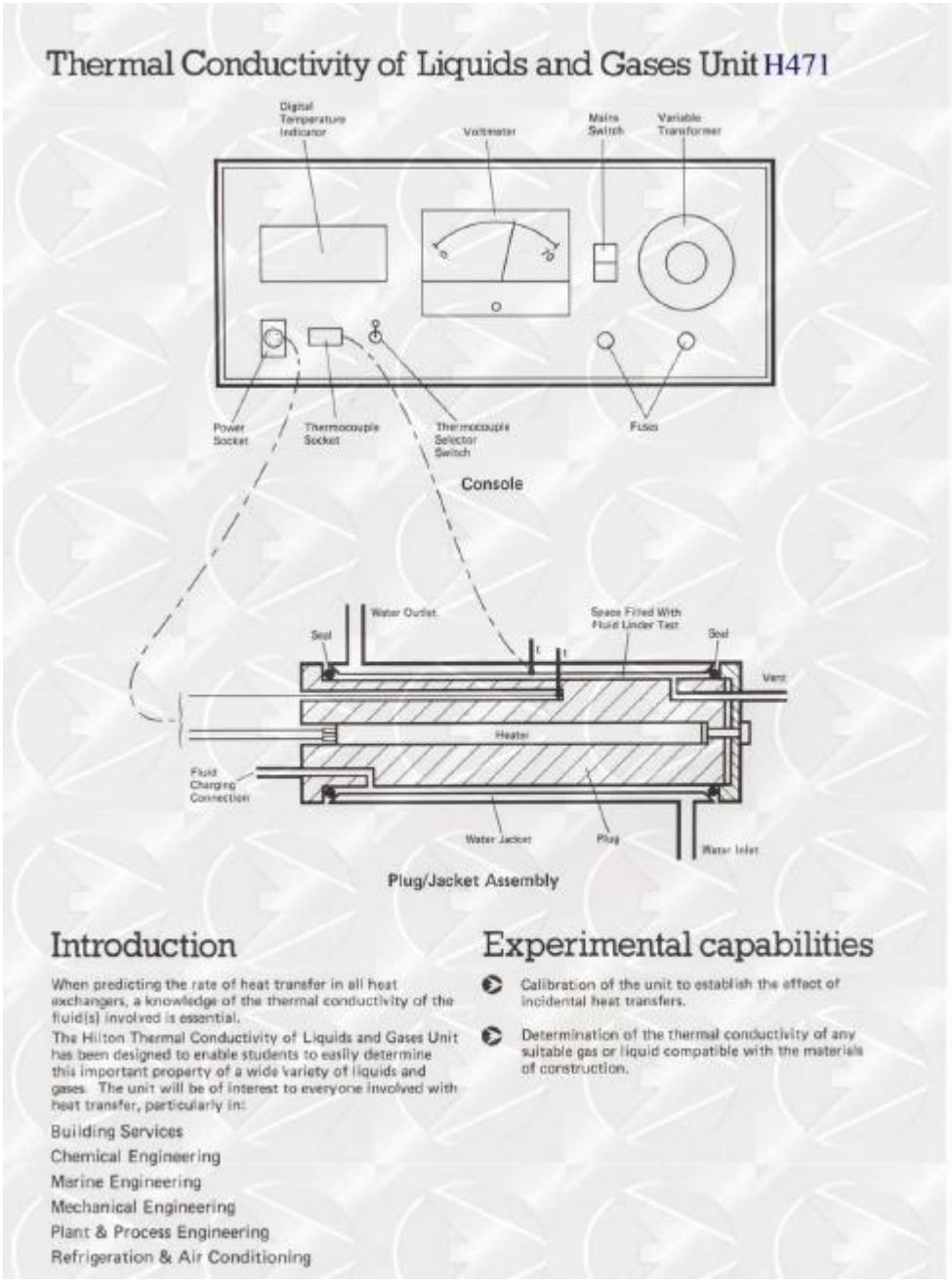

Figure 24: Schematic drawing of P.A. Hilton Thermal Conductivity of Liquids and Gases Unit H471

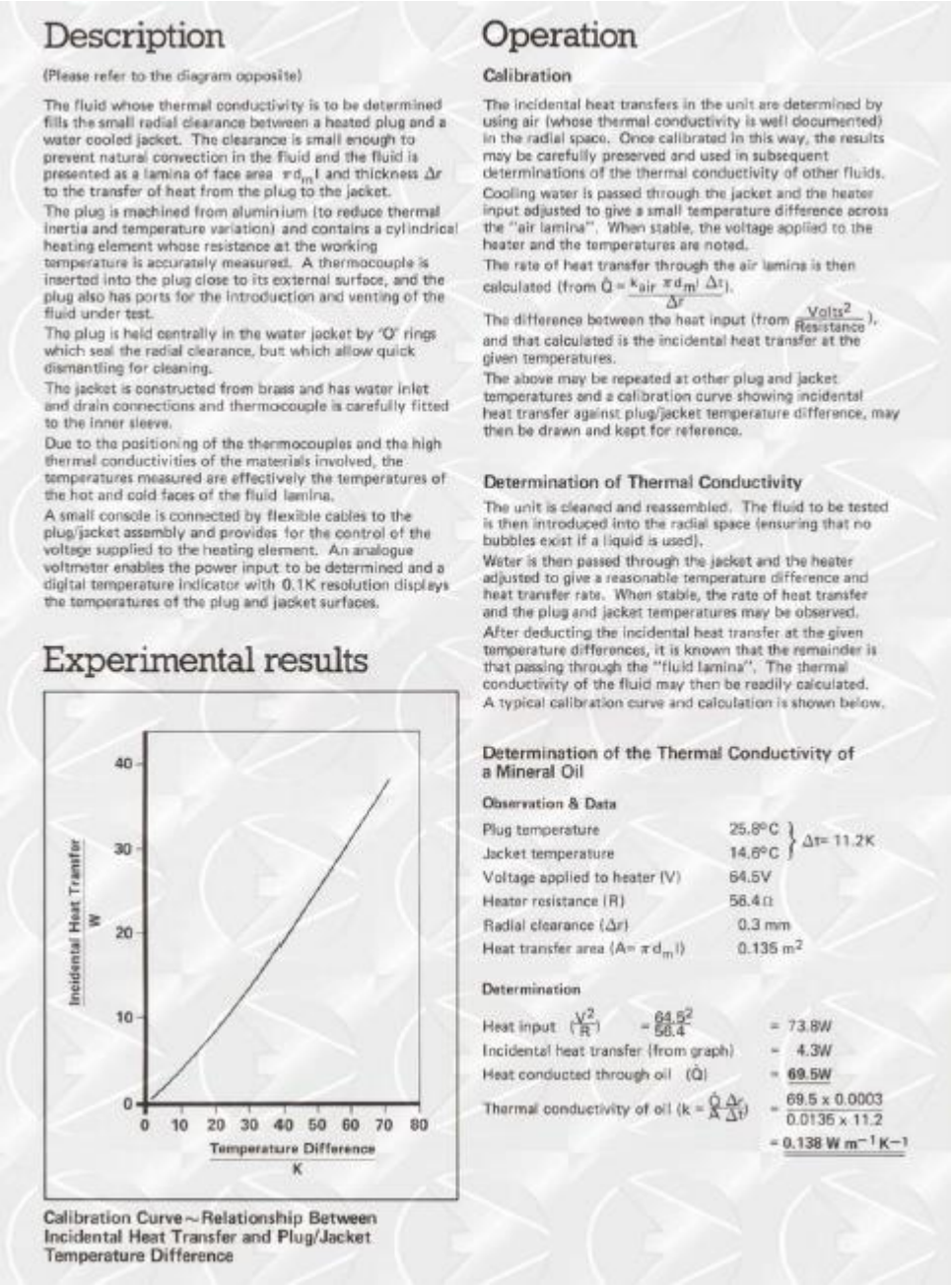

Description

(Please refer to the diagram opposite)

The fluid whose thermal conductivity is to be determined fills the small radial clearance between a heated plug and a water cooled jacket. The clearance is small enough to prevent natural convection in the fluid and the fluid is presented as a lamina of face area $\pi d_m l$ and thickness Δr to the transfer of heat from the plug to the jacket.

The plug is machined from aluminium (to reduce thermal inertia and temperature variation) and contains a cylindrical heating element whose resistance at the working temperature is accurately measured. A thermocouple is inserted into the plug close to its external surface, and the plug also has ports for the introduction and venting of the fluid under test.

The plug is held centrally in the water jacket by 'O' rings which seal the radial clearance, but which allow quick dismantling for cleaning.

The jacket is constructed from brass and has water inlet and drain connections and thermocouple is carefully fitted to the inner sleeve.

Due to the positioning of the thermocouples and the high thermal conductivities of the materials involved, the temperatures measured are effectively the temperatures of the hot and cold faces of the fluid lamina.

A small console is connected by flexible cables to the plug/jacket assembly and provides for the control of the voltage supplied to the heating element. An analogue voltmeter enables the power input to be determined and a digital temperature indicator with 0.1K resolution displays the temperatures of the plug and jacket surfaces.

Experimental results

Calibration Curve – Relationship Between Incidental Heat Transfer and Plug/Jacket Temperature Difference

Operation

Calibration

The incidental heat transfers in the unit are determined by using air (whose thermal conductivity is well documented) in the radial space. Once calibrated in this way, the results may be carefully preserved and used in subsequent determinations of the thermal conductivity of other fluids.

Cooling water is passed through the jacket and the heater input adjusted to give a small temperature difference across the "air lamina". When stable, the voltage applied to the heater and the temperatures are noted.

The rate of heat transfer through the air lamina is then calculated (from $\dot{Q} = \frac{k_{air}\, \pi d_m l\, \Delta t}{\Delta r}$).

The difference between the heat input (from $\frac{\text{Volts}^2}{\text{Resistance}}$), and that calculated is the incidental heat transfer at the given temperatures.

The above may be repeated at other plug and jacket temperatures and a calibration curve showing incidental heat transfer against plug/jacket temperature difference, may then be drawn and kept for reference.

Determination of Thermal Conductivity

The unit is cleaned and reassembled. The fluid to be tested is then introduced into the radial space (ensuring that no bubbles exist if a liquid is used).

Water is then passed through the jacket and the heater adjusted to give a reasonable temperature difference and heat transfer rate. When stable, the rate of heat transfer and the plug and jacket temperatures may be observed.

After deducting the incidental heat transfer at the given temperature differences, it is known that the remainder is that passing through the "fluid lamina". The thermal conductivity of the fluid may then be readily calculated.

A typical calibration curve and calculation is shown below.

Determination of the Thermal Conductivity of a Mineral Oil

Observation & Data

Plug temperature	25.8°C	Δt= 11.2K
Jacket temperature	14.6°C	
Voltage applied to heater (V)	64.5V	
Heater resistance (R)	58.4Ω	
Radial clearance (Δr)	0.3 mm	
Heat transfer area ($A = \pi d_m l$)	0.135 m^2	

Determination

Heat input $\left(\frac{V^2}{R}\right) = \frac{64.5^2}{58.4}$ = 73.8W

Incidental heat transfer (from graph) = 4.3W

Heat conducted through oil ($\dot{Q}$) = 69.5W

Thermal conductivity of oil $\left(k = \frac{\dot{Q}}{A}\frac{\Delta r}{\Delta t}\right) = \frac{69.5 \times 0.0003}{0.0135 \times 11.2}$

= 0.138 W $m^{-1} K^{-1}$

Figure 25: Sample calculation of thermal conductivity of sample liquid including incidental heat transfer calibration curve.